MICROSURGERY WILEY

Feasibility study of preoperative microvessel evaluation and characterization in perforator flaps using various modes of color-coded duplex sonography (CCDS)

Andreas Kehrer MD, PhD, FEBOPRAS[1] ⬤ | Daniel Lonic MD[1] |
Paul Heidekrueger MD, PhD[2] ⬤ | Talia Bosselmann MD[1] |
Christian D. Taeger MD, PhD[1] | Philipp Lamby MD, PhD[1] | Michael Kehrer MD[3] |
Ernst Michael Jung MD, PhD[4] | Lukas Prantl MD, PhD[1] |
Natascha Platz Batista da Silva MD[4]

[1]Department of Plastic, Hand and Reconstructive Surgery, University Hospital Regensburg, Germany

[2]Bogenhausen Hospital, Academic Teaching Hospital of Technical University Munich, Department of Plastic, Reconstructive, Hand and Burn Surgery, Germany

[3]Department of Trauma Surgery, University Hospital Bonn, Germany

[4]Department of Radiology, University Hospital Regensburg, Germany

Correspondence
Andreas Kehrer, Department of Plastic, Hand and Reconstructive Surgery, University Hospital Regensburg, Franz-Josef-Strauss-Allee 11, 93053 Regensburg, Germany
Email: andreaskehrer@gmx.de

Abstract

Background: Color-coded duplex sonography (CCDS) is useful for perforator flap design showing the highest sensitivity in identifying microvessels. This prospective study evaluates the feasibility of different ultrasound (US) modes applied by the microsurgeon in daily practice suggesting quantifiable reference values.

Methods: Twenty-four patients aged between 17 and 68 years (mean 43.3 ± 14.2 years) with 18 anterolateral thigh (ALT) and 6 superficial circumflex iliac artery (SCIP) flaps were included. Indications were traumatic ($n = 12$), infectious ($n = 6$), ischemic ($n = 4$), or tumor-associated defects ($n = 2$). Different US modes were evaluated regarding applicability using multifrequency linear probes (5–15 MHz). Vessels diameter, peak systolic velocity (PSV), end diastolic velocity (EDV), and resistance index (RI) were measured. Preoperative results were correlated to intraoperative findings.

Results: In the examined patient group with 24 perforator flaps a 100% correlation was seen when comparing perforators detected with CCDS/PD with intraoperative findings using optimized US settings. Sensitivity, PPV, and accuracy of CCDS were 100% respectively. Mean PSV of 16.99 ± 6.07 cm/s, mean EDV of 5.01 ± 1.84 cm/s and RI of 0.7 ± 0.07 were measured in microvessels (PW-mode). CCDS proved to be superior compared to PD in correct diameter assessment showing a mean diameter of 1.65 ± 0.45 mm, compared to PD-mode 1.31 ± 0.24 mm. Mean PSV and EDV were higher in ALT than in SCIP flaps, RI was slightly higher in SCIP flaps ($p > .05$). There were no significant differences in size of different flaps' perforators ($p > .05$).

Conclusion: CCDS represents a highly valuable tool in the daily practice of free flap reconstructions using optimized low flow US settings and multifrequency linear probes.

1 | INTRODUCTION

In the last decade, competencies of ultrasound (US)-guided micro-vessel visualization and blood flow imaging have improved immensely as US devices have enhanced in quality (Su et al., 2013; Tashiro et al., 2016). Visualization of microvascular structures has been a domain of color-coded duplex sonography (CCDS) and power Doppler (PD) because of their accuracy, repeatability, and portability. Furthermore, CCDS examinations are free of radiation exposure and are not dependent on contrast media. Overall availability, time, and cost savings are other important advantages of this fast-growing technology (Hayashi et al., 2019; Thomas et al., 2020; Visconti, Bianchi, Hayashi, & Salgarello, 2019; Visconti, Hayashi, Bianchi, & Salgarello, 2019).

High-resolution CCDS guided vascular flow imaging has proven as a potent instrument for microsurgeons in evaluating perforator vessels to simplify the design of perforator flaps in reconstructive surgery. Within the last few years, it has developed impetus and may spread faster than other modalities for detection and assessment of microvessels required for preoperative microvascular flap planning (Debelmas, Camuzard, Aguilar, & Qassemyar, 2018; Dorfman & Pu, 2014; Ensat et al., 2012; Feng et al., 2016; Gravvanis et al., 2010; Saito et al., 2011; Su et al., 2013). Anatomic and hemodynamic information may be provided in real-time imaging by CCDS of both vascular structures of the donor and recipient sites of flap reconstructions (Gravvanis, Petrocheilou, Tsoutsos, Delikonstantinou, & Karakitsos, 2013).

Specific US device programming and trimming is required and may tremendously enhance device sensitivity for detection of microvessels. A structured step-by-step approach for machine settings and perforator mapping sequences has been suggested previously by Kehrer et al. (2020).

CCDS is capable of combining modes for qualitative vessel visualization through overlaying color flow (CF) imaging of microvascular blood flow with gray scale US (B-mode) and pulse wave (PW)-mode. These modes are able to preoperatively identify perforators and measure hemodynamic parameters to simplify perforator vessel selection for perforator flap planning. PD offers the advantage of a more sensitive depiction of low flow vessels displaying the blood flow intensity in colors. However, PD is not capable of encoding the direction of blood flow, so that a differentiation of veins and arteries by PD only is impeded (Zwiebel, Pellerito, & Zwiebel, 2005). Although there are many different US techniques for optimized preoperative perforator evaluation, there are no common standards established for microsurgeons to perform the examinations nor are there any reference values to compare own findings to.

The following prospective study was designed to evaluate the feasibility of different US modes in daily practice of perforator flap planning. The focus was directed at the applicability of various US modes with respect to surgical decision-making. Thereby, representative diameter and flow measurements were gained to suggest comparable reference values from own clinical experiences.

2 | PATIENTS AND METHODS

The study was planned in accordance with the Helsinki Declaration of 1975. A vote of the local ethical committee was obtained (no. 18-1133-101) prior to study conduction. From August 2018 to August 2019, a group of 24 patients scheduled for perforator flap reconstructions performed at the Department of Plastic, Hand, and Reconstructive Surgery at the University Hospital Regensburg, Germany, was examined by an experienced examiner (Andreas Kehrer) using a comprehensive US examination protocol for flap planning. Written informed consent of the patients was obtained in each case. Free tissue transplants selected for reconstruction of soft tissue defects included anterolateral thigh (ALT) and superficial circumflex iliac artery (SCIP) perforator flaps. Recipient sites of the transplanted flaps were lower extremities, upper extremities and the temporal bone region. Preoperatively, perforator vessels were assessed with multiple US modes available for microvessel evaluation. Modes were evaluated regarding applicability for the purposes of US-based design of perforator flaps in a busy university hospital setting. B-mode, CCDS incl. PW-mode and PD-mode were used for perforator characterization. Quantitative parameters such as blood flow velocities and vascular diameter were determined at the deep fascia level. Peak systolic velocity (PSV), end diastolic velocity (EDV), and resistance index (RI) were measured in PW-mode (Video 1). Qualitative perforator assessment was focused at the same tissue layer using CCDS and PD. Skin projections of the perforators' emergence points (EP) at the deep fascia were marked preoperatively. The fundamental knobology of a standard control panel is illustrated in Figure 1. Subsequently, true microvessel anatomy and vessels' size were compared intra-operatively with preoperative US data (Figure 2 and Figure 4). Medial perforators were distinguished from lateral perforators in SCIP-flap procedures (Suh, Jeong, Choi, & Hong, 2017) (Figure 3). New generation high-resolution US devices (LOGIQ E9/GE, LOGIQ S7 XDclear, GE Healthcare, Milwaukee, Wisconsin) with different linear multi-frequency transducers, including a 12L-RS (5–13 MHz), a 9 L (6–9 MHz), and ML6-15-D (6–15 MHz) probe, as well as a convex probe C1-6D (1–6 MHz) for comparison reasons, were used. A standardized US protocol was applied in each case using B-mode US, CCDS incl. PW- and PD-modes.

Adequate basic settings of the US device to expedite detecting sizable perforators at the fascial level (emergence point) are shown in Table 1.

Statistical analysis was performed using t test, cross-tables, and descriptive statistics (SPSS, IBM). A p-value <.05 was considered statistically significant.

3 | RESULTS

A total number of 24 patients with 24 free perforator flaps including 18 ALT and 6 SCIP perforator flaps were examined in this study. The 15 male and 9 female patients were aged between 17 and 68 years (mean 43.3 ± 14.2 years). Indicators were traumatic extremity defects

in 12 cases and postoperative infections after primary surgery in 5 cases. One patient was treated after necrotizing fasciitis. Ischemic extremity (n = 4) defects were caused by diabetic foot syndrome or vasculitis. Tumor-associated defects after resection of a malignant melanoma and an arteriovenous malformation nidus lead to flap surgery in two cases. Recipient sites of the transplanted flaps were lower extremities in 20 cases, upper extremities in 3 cases and the temporal region in one case. Patient data, surgery indications, flap reconstructions, CCDS findings, and postoperative courses are shown in Table 2.

A clinical example of a CCDS guided suprafascial ALT-flap design is provided in Figure 4 (Video 2).

A 100% correlation was seen comparing perforators detected with CCDS or PD with intraoperative findings. No false-positive confirmation of microvessels was found. Sensitivity, PPV, and accuracy of CCDS and PD concerning a correct localization of perforator vessels were 100%.

An arterial signal at the emergence point was identified in PW-mode for every single perforator vessel detected. The mean overall
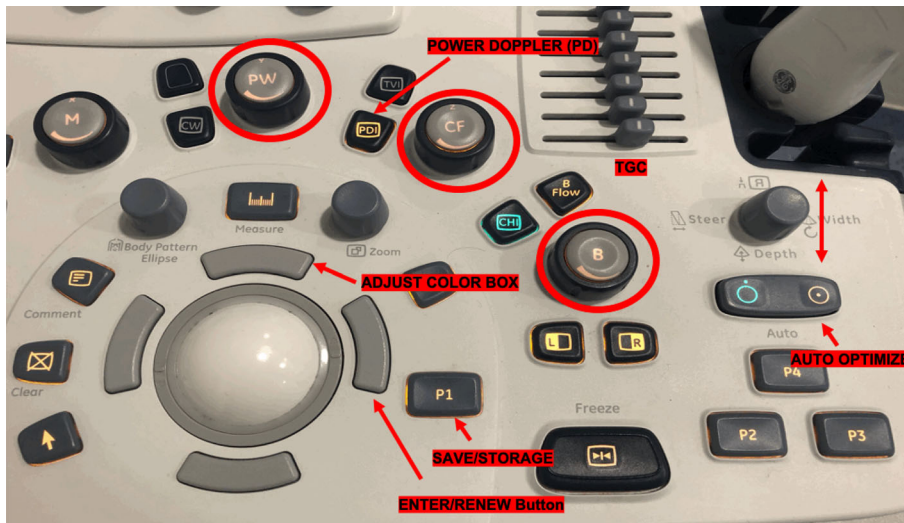

FIGURE 1 Basic knobology for the microsurgeon. Illustrated less obvious but important buttons for simplified usage. Different, suitable ultrasound (US) modes were indicated by red circles; PW-mode was usually initiated in color flow (CF)-mode. The time gain controls (TCG) was all set in a middle position. DEPTH was changed by upper and lower lever actions (far right, up). The AUTO OPTIMIZE button harmonized image quality. The ADJUST COLOR BOX button alternated the color box size in combination with the TRACKBALL. Using PW-mode, the ENTER/RENEW button (re)started flow velocity measurements. Button (P1) saved images (freezed) or cine loops (non-freezed short "videos") in this example

FIGURE 2 An example of color-flow perforator imaging in an anterolateral thigh (ALT)-flap procedure with intraoperative confirmation of a perforator at mid-thigh level (flap no. 13). Upper left: Color-flow ultrasound (US) enabled live visualization of microvessels in high imaging quality. In this ALT-flap design, preoperatively the superficial low flow perforator vessel could be imaged using color-coded duplex sonography (CCDS) from its emergence point (EP) at the deep fascia level up to the subdermal plexus. Its vascular course (higher flow in source vessels) through deeper muscle tissues was visualized simultaneously. Upper right: The EP has been marked on the skin and the flap design completed. The entire flap may then be circumcised. Lower left: The intrasurgically located target perforator corresponded exactly to its preoperative skin marking. Lower right: Flap 12 months after transfer

FIGURE 3 A color-coded duplex sonography (CCDS) measurement of blood flow velocities in a medial branch perforator of a free superficial circumflex iliac artery (SCIP) flap. The free tissue transfer was used to reconstruct a forefoot defect. Upper left: Quantitative values of hemodynamics were measured. In this medial branch SCIP-perforator first, an arterial signal was confirmed. It showed a peak systolic velocity of 9.9 cm/s (flap no. 23). Upper right: Small size full thickness defect of right forefoot (flap no. 21). Middle left: Preoperative skin marking of SCIP flap design. The EP and axis of the medial perforator were marked (vertical line just above inguinal crease). The flap design was completed before incision. Middle right: SCIP flap after inset showed adequate perfusion after transplantation to the dorsalis pedis vessels. Lower left and right: Flap healed 10 months post-op showing only moderate bulkiness

perforator PSV was 16.99 ± 6.07 cm/s, mean EDV was 5.01 ± 1.84 cm/s. A RI in perforator vessels of 0.7 ± 0.08 was calculated.

ALT-perforators (n = 18) showed a PSV of 17.02 ± 6.74 cm/s, EDV was 5.13 ± 1.90 cm/s. The mean RI in ALT perforator vessels was 0.69 ± 0.06.

In SCIP-perforators (n = 6), a PSV of 16.88 ± 4.77 cm/s and EDV of 4.65 ± 1.75 cm/s were measured. The RI in SCIP perforator vessels was 0.71 ± 0.1.

In every single perforator detected preoperatively, a positive evidence of pulsatility was confirmed intraoperatively. All perforator vessels targeted and skin-marked preoperatively were found to constitute suitable nourishing vessels for the perforator flaps and were included as the predominant supplying vessel in the flap pedicle, respectively.

The measured overall mean diameter of the examined perforators in CCDS mode was 1.65 ± 0.45 mm and correlated better to intraoperative findings in the majority of cases compared to PD. ALT perforator microvessels showed a mean diameter of 1.69 ± 0.47 mm compared to SCIP perforators with a mean of 1.55 ± 0.39 mm. The highly augmented signal of PD-mode was found to under- or over-estimate perforator vessels' size depending on the gain due to extra-vascular artifacts. When regulating the gain to spare out these artifacts in PD-mode, a mean diameter of perforator vessels of 1.31 ± 0.24 mm was documented overall. In contrast, with consequent device trimming microvessels could be visualized up to the subdermal

plexus with regular CF-mode displaying fewer extravascular artifacts and color-coding the blood flow direction. A differentiation of perforator artery from vein was possible with CF-mode in the majority of perforators, but not using PD-mode.

3.1 | Postoperative course and outcome

In 14 cases, the postoperative course was uneventful, and the flap reconstruction proved to be successful. In five cases, additional secondary split thickness skin grafting (STSG) was needed. Two free flaps were lost, thus a free radial forearm flap (n = 1) and a free latissimus dorsi flap (n = 1) were successfully used for salvage. Three cases with wound healing disorders healed on secondary intention.

3.2 | Statistical analysis

There were no significant differences in size (p > .05) of different flaps' perforators (mean ALT 1.69 mm vs. mean SCIP 1.55 mm). A trend close to significance was seen concerning the mean PSV and RI of patients with ALT and SCIP flaps: The PSV was higher in patients with ALT flaps (p = .06), whereas the RI proved to be lower in ALT patients (p = .08). Mean EDV showed no significant differences in ALT

FIGURE 4 Crush injury of the mid-hand featuring comminuted fractures accompanied by extended soft tissue loss in an obese patient. A reverse posterior interosseous (PIA) flap would have been a reconstructive option, however a free flap tailored to the defect was chosen (Video 2). Upper left: Figure 4 showed a suprafascial anterolateral thigh (ALT)-flap harvest using the hot−/ cold-zone dissection concept. Upper right: Although the patient (flap no. 12) was obese (BMI 37 kg/m^2) a thin flap could be raised. The dissection of the hot zone (blue marking) was slowed down to microsurgical preparation. Middle left/right: After inset the flap did not show excessive bulk. No secondary flap thinning procedures were necessary. An initial color mismatch resulted from a heavy teint in the upper body. The discrepancy resolved as expected some weeks later (see Video 2). Lower left and right: Situation 22 months post-operatively. Though the patient was offered a thinning procedure he was content with the functional outcome and refused any further surgeries

TABLE 1 CCDS settings for microvessel detection and evaluation

	Parameter	Recommendation	Presets	Comments
1	Probe selection	Linear	—	B-mode frequency 9–15 MHz, CCDS frequency medium to high
2	B-mode	Optimal contrasted image (lower gain levels)	Breast, thyroid, vascular	Further modification of parameters
4	PRF/scale	Low Doppler 0.5–20 Hz, CCDS 3–10 cm/s	Variable	At threshold to or showing mild intravascular aliasing
5	Color gain	High (15–30)	Depending on preset	B-mode: 25–45, CF-mode 10–20 (at threshold but below showing extravascular artifacts)
6	Power Doppler (PD) mode	Small microvessels	—	Increases sensitivity 3–5×, more artifacts
7	Wall filter	Low or turned off	<50 Hz	If set too high low flow signals are eliminated

Note: Table with suitable basic settings of the ultrasound device to expedite detecting sizable perforators at the fascial level (emergence point).

and SCIP patients ($p > .05$). In the studied patient, collective perforators' diameter measured in CCDS proved to be more accurate compared to PD measurements showing a trend close to significance ($p = .08$).

4 | DISCUSSION

A systematic review by Cheng et al. comparing hand-held Doppler, CCDS, and CT angiography revealed that CCDS had the highest

TABLE 2 Patients' data, indication, flap reconstructions, and CCDS findings

Flap. No.	Pat. age	Gender	Location of defect	Surgery indication	Flap	Perforator	Perforator confirmed intraoperatively	Target perforator used	Perforator diameter (mm)	PSV cm/s	EDV cm/s	RI	Postoperative course/ complications	Final outcome
1	21	M	Forefoot	Lawnmower accident, fractures, tendon lacerations	ALT	B-perforator	Yes	Yes	1.5	12.4	4	0.76	Uneventful	Success
2	47	F	Ankle	Crural ulcer after fracture of ankle joint (20 years previously)	ALT	B-perforator	Yes	Yes	2.5	33.4	8.8	0.74	Wound dehiscence, STSG	Success
3	53	M	Distal tibia	Crural ulcer after chainsaw injury (10 years previously)	ALT	B-perforator	Yes	Yes	1.9	10.1	2.8	0.72	Uneventful	Success
4	47	F	Ankle	Infected hematoma	ALT	B-perforator	Yes	Yes	1.2	9.6	2.7	0.72	Partial flap loss, STSG	Success
5	39	M	Forefoot	Crush avulsion injury	ALT	B-perforator	Yes	Yes	2.8	10.7	3.8	0.64	Uneventful	Success
6	46	M	Ankle	Diabetic foot	ALT	B-perforator	Yes	Yes	1.3	13.8	4.0	0.71	Flap loss, venous thrombosis	Free latissimus dorsi flap for salvage
7	57	M	Forefoot	Diabetic foot	ALT	A-perforator	Yes	Yes	1.7	20.6	4.8	0.77	Wound dehiscence, STSG	Success
8	29	M	Forearm	Vehicle rollover accident	ALT	B-perforator	Yes	Yes	1.8	28.4	9.8	0.65	Wound healing disorder, healed on secondary intention	Success
9	58	F	Forearm, palmar	Necrotizing fasciitis	ALT	B-perforator	Yes	Yes	1.2	20.6	5.2	0.7	Wound dehiscence, STSG	Success
10	25	M	Forefoot	Crush avulsion injury	ALT	B-perforator	Yes	Yes	1.4	16.9	7.7	0.55	Uneventful	Success
11	32	F	Forefoot	Arterio-venous malformation	ALT	B-perforator	Yes	Yes	1.6	18.0	5.5	0.7	Partial flap loss, STSG	Success
12	53	F	Hand	Crush avulsion injury	ALT	B-perforator	Yes	Yes	1.7	24.4	5.6	0.7	Uneventful	Success
13	19	M	Distal tibia	Crush avulsion injury	ALT	B-perforator	Yes	Yes	2.4	14.6	5.9	0.60	Uneventful	Success
14	54	M	Foot sole	Malignant melanoma	ALT	B-perforator	Yes	Yes	1.2	16.3	4.8	0.71	Wound healing disorder, revision for contouring flap, healed on secondary intention	Success
15	52	F	Temporal region	Infection after skull bone implant	ALT	A-perforator	Yes	Yes	1.6	21.7	5.1	0.76	Flap loss, venous thrombosis	Free radial forearm flap for salvage
16	66	M	Ankle	Infection after Achilles tendon repair	ALT	B-perforator	Yes	Yes	1.3	10.6	3.3	0.70	Uneventful	Success
17	32	M	Forefoot	Motor bike accident	ALT	B-perforator	Yes	Yes	1.2	10.9	3.4	0.69	Uneventful	Success
18	38	F	Tibia	Crush avulsion injury	ALT	B-perforator	Yes	Yes	2.1	13.5	5.3	0.61	Uneventful	Success
19	47	F	Ankle	Crush avulsion injury	SCIP	Medial	Yes	Yes	1.3	14.7	3.1	0.79	Uneventful	Success
20	58	M	Forefoot	Diabetic foot	SCIP	Medial	Yes	Yes	1.7	24.5	6.8	0.72	Uneventful	Success

(Continues)

TABLE 2 (Continued)

Flap. No.	Pat. age	Gender	Location of defect	Surgery indication	Flap	Perforator	Perforator confirmed intraoperatively	Target perforator used	Perforator diameter (mm)	PSV cm/s	EDV cm/s	RI	Postoperative course/ complications	Final outcome
21	68	M	Forefoot	Vasculitis	SCIP	Medial	Yes	Yes	1.2	17.9	5.7	0.68	Wound healing disorder due to vasculitis, healed on secondary intention	Success
22	17	F	Ankle	Motor bike accident	SCIP	Medial	Yes	Yes	2.3	16.4	2.1	0.87	Uneventful	Success
23	43	M	Ankle	Crush avulsion injury	SCIP	Medial	Yes	Yes	1.6	9.9	4.5	0.55	Uneventful	Success
24	56	M	Forefoot	Crush avulsion injury	SCIP	Medial	Yes	Yes	1.2	17.9	5.7	0.68	Uneventful	Success

Notes: This table showed the patients' basic data including age, gender, side of defect, indications leading to flap reconstruction as well as the postoperative course. The characterization of perforators included qualitative and quantitative parameters. Diameter (mm) of perforators at the deep fascia level was measured in color flow (CF)-mode. Values for blood flow assessment included peak systolic velocity (PSV) in cm/s, end diastolic velocity (ED) in cm/s and resistance index (RI). These parameters were measured in pulse wave (PW)-mode.
Abbreviation: STSG, split thickness skin graft.

pooled sensitivity of 95.7% as well as the highest pooled predictive value of 94.3% to identify microvessels for perforator flaps such as the ALT flap (Cheng, Lin, & Chang, 2012a, 2012b, 2013). Thomas et al. (2020) confirmed the superiority of CCDS to conventional Doppler US for perforator mapping and characterization prior to ALT flap harvest. Kehrer et al. showed that sensitivity of PD for microvessel detection was 96.7% with a mean distance from the emergence point (true anatomy) to the projected preoperative skin marking after PD mapping (assumed anatomy) of 2.45 ± 1.90 mm (0–6 mm) (Kehrer, Hsu, Chen, Sachanandani, & Tsao, 2018). These findings could be confirmed by the results of this study proving a 100% sensitivity rate for CCDS guided perforator detection although CCDS proved to be superior compared to PD in correct assessment of microvessel diameter.

However, there have not been studies focusing on the optimized device settings for high quality CCDS and PW application. Therefore, the novelty of our study data is the presentation of specific information for the microsurgeon on the exact settings of duplex US and PW for perforator detection and characterization, which has not been described in detail before.

Multifrequency linear transducers proved to be favorable for superficial microvessel characterization whereas convex (curved typed) probes were found less suitable. The higher frequency linear probes 12L-RS (5–13 MHz) and ML6-15D (6–15 MHz) showed superior imaging qualities than the linear 9L (6–9 MHz) transducer with lower US frequencies. Selection of the "breast" preset program provided the best overall contrast of the B-mode picture and optimized color-flow presettings for microvessel interpretation. Relevant settings to optimize the CF-mode image were adjustment of CF-mode frequency, pulse-repetition frequency (PRF)/scale, color gain, color box size, angular correction/steer for color box orientation, and usage of the invert-button. Key steps to fine-tune PW-mode image were sample volume adjustment, angular correction, PRF/scale and base line correction. The renew calculation button, invert button, and switching on the automatic value calculation of the freezed image greatly helped to speed up blood flow diagnostics and the "measure" button was used to determine microvessel diameter. Inserting patient data before saving images/cine loops and adjusting body pattern pictograms and possibly text edit findings on the screen improved subsequent interpretation of images at a later date.

The entire body of microvessels detected by CCDS and confirmed by surgical dissection was sizable. The finally used skin perforators provided a diameter of 1.69 mm in ALT and 1.55 mm in SCIP flaps, though our findings showed that usable perforators may be sized to a minimum of 0.9 mm. These results differed slightly from suggestions of recent literature proposing minimal diameters of >0.5 mm as suitable (Lin et al., 2008; Miller, Potparic, Colen, Sorrell, & Carraway, 1995).

Not only microvessels' diameter, but also blood flow characteristics may influence operation's outcome. However, other author groups before have not described reproducible values in detail, although it was reported that specific qualifications for perforator assessment were finally attributed to CCDS and PW-mode. Abnormal or abundant vascular anatomy of perforator flaps such as the ALT flap

have been described and may be detected preoperatively with CCDS (Hong et al., 2010; Hsieh, Yang, Chen, Kuo, & Jeng, 2009; Lu et al., 2015). The superficial fascial plane harvest of thin perforator flaps has been popularized by Hong et al. refining function and cosmesis of recipient and donor sites (Hong et al., 2014; Hong & Chung, 2013). Hong et al. (2014) have also popularized a superficial flap harvest using a "hot-zone/cold-zone" dissection concept. As a prerequisite, the suprafascial perforator architecture has to be known before incision to locate the perforator at a level within the subcutaneous tissue layer. It requires reliable CCDS-guided preoperative diagnostics. Perforator flaps are now widely performed in reconstructive surgery. Nevertheless, astonishing little knowledge exists of the altered hemodynamics within these flaps before and following transplantation. Therefore, another novelty of this study was to describe reproducible and comparable flow parameters of perforator vessels, which has not been focus of other author groups before. Ulatowski (2012) presented quantitative blood flow parameters of perforators in their study, but missed out describing the basic settings and the use of an angle correction. Therefore, we figured that reproducibility and comparability were not sufficiently given. Blood velocity in a perforator artery was shown to be higher than the one found in the original vascular source vessel (Saba et al., 2013). Some effects of the enhanced blood flow velocity within these microvessels and the subordinated cutaneous microcirculation of perforator flaps have been studied (Saba et al., 2013), although no standard references values could be established yet. Our findings proposed further measurement values of diameter, PSV, EDV, and RI as representative parameters of size and hemodynamics, which can be used for initial comparison reasons. Nevertheless, larger prospective studies are required to establish generally applicable reference values for CCDS guided choice of suitable perforator microvessels.

CF-mode constitutes the standard color-coding mode and superimposes a color box window on the B-mode image in which Doppler information is displayed in color coded vascular flow. The color visualizes blood flow direction in relation to the probe. Color intensity (or gain) reflects flow velocity. Pulsatile blood flow piercing the deep fascia level is indicative for perforator vessel anatomy. With adequate device trimming, this mode simplifies detection and evaluation of microvessels' perforator at the deep fascia and quantification of measurements are possible. Application of PD-mode enhances sensitivity by a factor of 3 to 5 compared to CF-mode (Naqvi & Perese, 2013) and displays the intensity and velocity of blood flow with substantial amplification. However, a differentiation of perforator artery and vein is not possible and extravascular flow signals around detected perforators are commonly faced impeding realistic vessel diameter judgment. Even though it multiplies device sensitivity for detection of microvessels, PD-mode therefore showed some short comings for realistic perforator appreciation. In most situations, it was found to be unnecessary because with consequent device trimming microvessels could be visualized up to the subdermal plexus with regular non-augmented CF-mode. PD-mode could possibly further lead to an overestimation of tiny microvessels which could not suitable for supplying mid-size to large angiosomes. This finding has also been described in the context of microvessel mapping in the design of profunda artery perforator flaps previously (Kehrer et al., 2018). With specific device settings for detection of low-flow, in our hands PD-mode has lost its past supremacy to visualize microvessels as now CF-mode performs more reliably in this matter.

Deliberately, we set a focus of our evaluation on the applicability of CCDS for the purposes of CCDS-based design of perforator flaps in a regular busy university hospital setting. Time constraints faced by the present clinical workload require a focused approach to CCDS. A selection of only the modes with the highest level of significance for clinical purposes is favorable. If individual perforator evaluation would include every existing mode and respect all modalities available by modern US technology, a reasonable time-value proportion would be compromised.

CCDS perforator evaluation has been evolved to become a key element in our flap planning. After several years of applying US technology in our practice CCDS has found to be convenient, flexible, inexpensive, and quickly repeatable. Fundamental aspects of CCDS guided perforator assessment were identified by application of a standardized approach. Appropriate device configurations for improved perforator imaging have been described by our team previously. We found that a preoperative CCDS exam scheduled the day before surgery is advantageous and relaxes the microsurgeon to perform the operation on the day of surgery at the ease of already knowing the exact location of the perforator(s) targeted. Microvessel size and location influenced surgical decision-making more than hemodynamic values, though a most favorable diameter should be determined by further studies with larger patient populations. Perforator selection by the microsurgeon is usually dependent on a multitude of factors as intended pedicle length, patient positioning on the OR table, topographical ease of dissection, possibly present previous surgery sites, tissue thickness, surgeon's experience, and many more. Interestingly, in this series of flaps perforator choice was based rather on diameter and location and was less dependent on flow measurements. An arterial signal was identified preoperatively in every perforator vessel located and confirmed by attention to pulsatility intraoperatively. Findings of the group of Hong et al. and Lin et al. suggested that the recipient artery may be utilized if the PSV is greater than 15 to 20 cm/s which could be confirmed by own findings with mean PSV of 16.99 cm/s in perforator vessels overall. (Hong et al., 2014; Hong & Chung, 2013; Lin et al., 2008) When planning perforator to perforator anastomosis in flaps, their data suggest matching PSVs of pedicle with recipient vessels (Suh et al., 2016). High-resolution ultrasonography is capable to identify vascular structures as small as 0.18 to 0.2 mm in diameter (Schwabegger, Bodner, Rieger, Jaschke, & Ninkovic, 1999; Stupp, Pavlidis, Busse, & Thanos, 2004). Other cross-sectional imaging techniques, for example, CT, are limited to a minimal slice thickness of 0.5 mm (Boucher et al., 2013). Reliable preoperative comprehension of perforator anatomy shortens flap harvest time, overall operative time, and enhances outcomes of complex reconstructions (Kehrer et al., 2020). CCDS microvessel mapping enhances perforator flap designs by capturing dominant vessels and maximizing flap survival (Rand, Cramer, &

Strandness Jr., 1994). CCDS has also shown its significance for post-operative evaluation of flap tissue perfusion monitoring flaps (Kehrer et al., 2017). Future perspectives comprise 3D microvessel imaging CCDS as well as contrast-enhanced US-guided imaging of microcirculation in flaps (Sidhu et al., 2018; Su et al., 2013).

Preoperative perforator evaluation with CCDS comes at some cost of time which may be problematic in a busy plastic surgical practice of a steadily growing unit as the one presenting this study. However, time invested for CCDS guided microvessel seemed to pay off for the authors by far, regarding the ease of not having to surgically detect target perforators and at the gain of having an already finalized flap design even before the first incision. This relaxation of the reconstructive surgeon often aided the authors in focusing on other important details of the reconstructions performed and led to more extensive, higher quality and foremost a combination of reconstructive steps all-in-one operation. Comparable results were reported by Thomas et al., who proved the time and cost efficiency of CCDS over conventional Doppler sonography due to perforator mapping preoperatively. They reported a reduction of about 73 min in harvesting time and of up to 90 min in operating time if CCDS guided perforator assessment was performed preoperatively (Thomas et al., 2020). This circumstance may not be underestimated as a combination of different reconstructive steps may help to save hospitalization time, costs and resources. It very well may result in earlier reconvalescence and rehabilitation of the patient as well as a better overall outcome.

5 | CONCLUSION

Application of selective CCDS mode in preoperative perforator vessel assessment simplifies suitable microvessel selection in perforator flap designs compared to other US modes. CCDS represents a feasible and highly valuable tool in the daily practice of free flap reconstructions providing qualitative and quantitative vessel information considering size and hemodynamics.

AUTHOR CONTRIBUTIONS
All authors meet the required conditions for authorship: (a) substantial contributions to conception and design, acquisition of data, or analysis and interpretation of data; (b) drafting the article or revising it critically for important intellectual content; (c) final approval of the version to be published; and (d) agreement to be accountable for all aspects of the work in ensuring that questions related to the accuracy or integrity of any part of the work are appropriately investigated and resolved.

ORCID
Andreas Kehrer https://orcid.org/0000-0001-9472-7662
Paul Heidekrueger https://orcid.org/0000-0002-4656-3808

REFERENCES

Boucher, F., Moutran, M., Boutier, R., Papillard, M., Rouviere, O., Braye, F., & Mojallal, A. (2013). Preoperative computed tomographic angiography and perforator flaps: A standardization of the protocol. *Annales de Chirurgie Plastique et Esthétique*, 58(4), 290–309.

Cheng, H. T., Lin, F. Y., & Chang, S. C. (2012a). Diagnostic efficacy of preoperative 64-section multidetector computed tomographic angiography in identifying the cutaneous perforators in the anterolateral thigh flap: An evidence-based review. *Plastic and Reconstructive Surgery*, 130(5), 771e–772e.

Cheng, H. T., Lin, F. Y., & Chang, S. C. (2012b). Evaluation of diagnostic accuracy using preoperative handheld Doppler in identifying the cutaneous perforators in the anterolateral thigh flap: A systematic review. *Plastic and Reconstructive Surgery*, 129(4), 769e–770e.

Cheng, H. T., Lin, F. Y., & Chang, S. C. (2013). Diagnostic efficacy of color Doppler ultrasonography in preoperative assessment of anterolateral thigh flap cutaneous perforators: An evidence-based review. *Plastic and Reconstructive Surgery*, 131(3), 471e–473e.

Debelmas, A., Camuzard, O., Aguilar, P., & Qassemyar, Q. (2018). Reliability of color Doppler ultrasound imaging for the assessment of anterolateral thigh flap perforators: A prospective study of 30 perforators. *Plastic and Reconstructive Surgery*, 141(3), 762–766.

Dorfman, D., & Pu, L. L. (2014). The value of color duplex imaging for planning and performing a free anterolateral thigh perforator flap. *Annals of Plastic Surgery*, 72(Suppl 1), S6–S8.

Ensat, F., Babl, M., Conz, C., Rueth, M. J., Greindl, M., Fichtl, B., … Spies, M. (2012). The efficacy of color duplex sonography in preoperative assessment of anterolateral thigh flap. *Microsurgery*, 32(8), 605–610.

Feng, S., Min, P., Grassetti, L., Lazzeri, D., Sadigh, P., Nicoli, F., … Zhang, Y. X. (2016). A prospective head-to-head comparison of color Doppler ultrasound and computed tomographic angiography in the preoperative planning of lower extremity perforator flaps. *Plastic and Reconstructive Surgery*, 137(1), 335–347.

Gravvanis, A., Karakitsos, D., Dimitriou, V., Zogogiannis, I., Katsikeris, N., Karabinis, A., & Tsoutsos, D. (2010). Portable duplex ultrasonography: A diagnostic and decision-making tool in reconstructive microsurgery. *Microsurgery*, 30(5), 348–353.

Gravvanis, A., Petrocheilou, G., Tsoutsos, D., Delikonstantinou, I., & Karakitsos, D. (2013). Integrating imaging techniques in lower limb microsurgical reconstruction: Focusing on ultrasonography versus computed tomography angiography. *In Vivo*, 27(3), 371–375.

Hayashi, A., Giacalone, G., Yamamoto, T., Belva, F., Visconti, G., Hayashi, N., … Salgarello, M. (2019). Ultra high-frequency ultrasonographic imaging with 70 MHz scanner for visualization of the lymphatic vessels. *Plastic and Reconstructive Surgery. Global Open*, 7(1), e2086.

Hong, J. P., Choi, D. H., Suh, H., Mukarramah, D. A., Tashti, T., Lee, K., & Yoon, C. (2014). A new plane of elevation: The superficial fascial plane for perforator flap elevation. *Journal of Reconstructive Microsurgery*, 30(7), 491–496.

Hong, J. P., & Chung, I. W. (2013). The superficial fascia as a new plane of elevation for anterolateral thigh flaps. *Annals of Plastic Surgery*, 70(2), 192–195.

Hong, J. P., Kim, E. K., Kim, H., Shin, H. W., Hwang, C. H., & Lee, M. Y. (2010). Alternative regional flaps when anterolateral thigh flap perforator is not feasible. *Journal of Hand and Microsurgery*, 2(2), 51–57.

Hsieh, C. H., Yang, J. C., Chen, C. C., Kuo, Y. R., & Jeng, S. F. (2009). Alternative reconstructive choices for anterolateral thigh flap dissection in cases in which no sizable skin perforator is available. *Head & Neck*, 31(5), 571–575.

Kehrer, A., Heidekrueger, P. I., Lonic, D., Taeger, C. D., Klein, S., Lamby, P., … Batista da Silva, N. P. (2020). High-resolution ultrasound-guided perforator mapping and characterization by the microsurgeon in lower limb reconstruction. *Journal of Reconstructive Microsurgery*. https://doi.org/10.1055/s-0040-1702162

Kehrer, A., Hsu, M. Y., Chen, Y. T., Sachanandani, N. S., & Tsao, C. K. (2018). Simplified profunda artery perforator (PAP) flap design using power Doppler ultrasonography (PDU): A prospective study. *Microsurgery*, *38*(5), 512–523.

Kehrer, A., Mandlik, V., Taeger, C., Geis, S., Prantl, L., & Jung, E. M. (2017). Postoperative control of functional muscle flaps for facial palsy reconstruction: Ultrasound guided tissue monitoring using contrast enhanced ultrasound (CEUS) and ultrasound elastography. *Clinical Hemorheology and Microcirculation*, *67*(3–4), 435–444.

Kehrer, A., Sachanadani, N. S., da Silva, N. P. B., Lonic, D., Heidekrueger, P., Taeger, C. D., ... Hong, J. P. (2020). Step-by-step guide to ultrasound-based design of alt flaps by the microsurgeon—Basic and advanced applications and device settings. *Journal of Plastic, Reconstructive & Aesthetic Surgery*, *73*(6), 1081–1090.

Lin, C. T., Huang, J. S., Hsu, K. C., Yang, K. C., Chen, J. S., & Chen, L. W. (2008). Different types of suprafascial courses in thoracodorsal artery skin perforators. *Plastic and Reconstructive Surgery*, *121*(3), 840–848.

Lu, J. C., Zelken, J., Hsu, C. C., Chang, N. J., Lin, C. H., Wei, F. C., & Lin, C. H. (2015). Algorithmic approach to anterolateral thigh flaps lacking suitable perforators in lower extremity reconstruction. *Plastic and Reconstructive Surgery*, *135*(5), 1476–1485.

Miller, J. R., Potparic, Z., Colen, L. B., Sorrell, K., & Carraway, J. H. (1995). The accuracy of duplex ultrasonography in the planning of skin flaps in the lower extremity. *Plastic and Reconstructive Surgery*, *95*(7), 1221–1227.

Naqvi, T. Z., & Perese, S. (2013). Noninvasive vascular appropriateness criteria—Review and comments on the American College of Cardiology (ACC) guidelines. *Journal of the American Society of Echocardiography*, *26*(5), A34.

Rand, R. P., Cramer, M. M., & Strandness, D. E., Jr. (1994). Color-flow duplex scanning in the preoperative assessment of TRAM flap perforators: A report of 32 consecutive patients. *Plastic and Reconstructive Surgery*, *93*(3), 453–459.

Saba, L., Atzeni, M., Rozen, W. M., Alonso-Burgos, A., Bura, R., Piga, M., & Ribuffo, D. (2013). Non-invasive vascular imaging in perforator flap surgery. *Acta Radiologica*, *54*(1), 89–98.

Saito, A., Furukawa, H., Hayashi, T., Oyama, A., Funayama, E., & Yamamoto, Y. (2011). Intraoperative color Doppler sonography in the elevation of anterolateral thigh flap. *Microsurgery*, *31*(7), 582–583.

Schwabegger, A. H., Bodner, G., Rieger, M., Jaschke, W. R., & Ninkovic, M. M. (1999). Internal mammary vessels as a model for power Doppler imaging of recipient vessels in microsurgery. *Plastic and Reconstructive Surgery*, *104*(6), 1656–1665.

Sidhu, P. S., Cantisani, V., Dietrich, C. F., Gilja, O. H., Saftoiu, A., Bartels, E., ... Wijkstra, H. (2018). The EFSUMB guidelines and recommendations for the clinical practice of contrast-enhanced ultrasound (CEUS) in non-hepatic applications: Update 2017 (short version). *Ultraschall in der Medizin*, *39*(2), 154–180.

Stupp, T., Pavlidis, M., Busse, H., & Thanos, S. (2004). Presurgical and postsurgical ultrasound assessment of lacrimal drainage dysfunction. *American Journal of Ophthalmology*, *138*(5), 764–771.

Su, W., Lu, L., Lazzeri, D., Zhang, Y. X., Wang, D., Innocenti, M., ... Messmer, C. (2013). Contrast-enhanced ultrasound combined with three-dimensional reconstruction in preoperative perforator flap planning. *Plastic and Reconstructive Surgery*, *131*(1), 80–93.

Suh, H. S., Jeong, H. H., Choi, D. H., & Hong, J. P. (2017). Study of the medial superficial perforator of the superficial circumflex iliac artery perforator flap using computed tomographic angiography and surgical anatomy in 142 patients. *Plastic and Reconstructive Surgery*, *139*(3), 738–748.

Suh, H. S., Oh, T. S., Lee, H. S., Lee, S. H., Cho, Y. P., Park, J. R., & Hong, J. P. (2016). A new approach for reconstruction of diabetic foot wounds using the angiosome and supermicrosurgery concept. *Plastic and Reconstructive Surgery*, *138*(4), 702e–709e.

Tashiro, K., Yamashita, S., Araki, J., Narushima, M., Iida, T., & Koshima, I. (2016). Preoperative color Doppler ultrasonographic examination in the planning of thoracodorsal artery perforator flap with capillary perforators. *Journal of Plastic, Reconstructive & Aesthetic Surgery*, *69*(3), 346–350.

Thomas, B., Warszawski, J., Falkner, F., Nagel, S. S., Schmidt, V. J., Kneser, U., & Bigdeli, A. K. (2020). A comparative study of preoperative color-coded Duplex ultrasonography versus handheld audible Dopplers in ALT flap planning. *Microsurgery*, *40*(5), 561–567.

Ulatowski, L. (2012). Colour Doppler assessment of the perforators of anterolateral thigh flap and its usefulness in preoperative planning. *Polski Przegląd Chirurgiczny*, *84*(3), 119–125.

Visconti, G., Bianchi, A., Hayashi, A., & Salgarello, M. (2019). Pure skin perforator flap direct elevation above the subdermal plane using preoperative ultra-high frequency ultrasound planning: A proof of concept. *Journal of Plastic, Reconstructive & Aesthetic Surgery*, *72*, 1700–1738.

Visconti, G., Hayashi, A., Bianchi, A., & Salgarello, M. (2019). Technological advances in lymphatic surgery: The emerging role of ultrasound. *Plastic and Reconstructive Surgery*, *144*, 940e–942e.

Zwiebel, W. J., Pellerito, J. S., & Zwiebel, W. J. (2005). *Introduction to vascular ultrasonography* (Vol. xvi, p. 723). Philadelphia, PA: Elsevier Saunders.

SUPPORTING INFORMATION

Additional supporting information may be found online in the Supporting Information section at the end of this article.